PCCP COMMUNICATION

Phase equilibria of water in cylindrical nanopores

Ivan Brovchenko,[a] Alfons Geiger*[a] and Alla Oleinikova[b]

[a] *Physikalische Chemie, Universität Dortmund, 44221 Dortmund, Germany*
[b] *Physikalische Chemie, Ruhr-Universität Bochum, 44780 Bochum, Germany*

Received 26th January 2001, Accepted 22nd March 2001
First published as an Advance Article on the web 5th April 2001

Phase equilibria of water in cylindrical nanopores were simulated in the Gibbs ensemble. The decrease of the critical temperature in the confinement compared to the bulk value attains 35% in the pores with radius $R_c = 12$ Å. The shape of the coexistence curve changes strongly with an increasing water–substrate interaction. This is found to be the result of a crossover from 3D surface to 2D behaviour in the surface layer. At the strongest water–substrate interactions of our study up to 3 coexistence curves are observed due to layering transitions.

The properties of fluids in confining geometries are an area of intense experimental and theoretical research and computer simulations. Molecular systems confined within narrow pores with sizes of a few molecular diameters in some directions exhibit physical properties which differ significantly from those in the bulk. Strong shifts of the liquid–vapour critical temperature and density due to the confinement of the fluids were observed experimentally in nanoporous materials (see review[1] and references therein). In particular, experimental studies of capillary condensation of some simple gases in perfect unconnected cylindrical pores with a radius of 12 Å show pore critical temperatures 30–35% below the bulk values.[2]

The rare experimental studies of the shape of the coexistence curve of confined fluids[3–7] show essential variations of its shape, but the accuracy of these experimental results is rather low. In a wide temperature range this shape varies from triangle-like for fluids in porous glasses to rectangular-like with a flat top for fluids in active carbon.[3] An analysis of the top of the coexistence curve of confined fluids gives an exponent β, which characterizes its shape, of about 0.3 for aerogels[4,5] and around 0.5 for porous glasses.[6]

A fluid which is confined in an infinite cylindrical pore may be considered to be close to a one dimensional system and thus it should not exhibit a true liquid–vapour critical point at temperatures above 0 K. However, first order phase transitions were observed to be only slightly rounded in narrow cylindrical pores. The separate phases appear as a succession of alternating domains of liquid and gas along the pore axis.[8] The critical temperature T_c in a cylindrical pore thus could be defined as the temperature above which the two microphases become indistinguishable.

The first order phase transition was found to be rather sharp even in cylindrical pores with a radius of 2.5 molecular diameters both in density functional theory calculations[9] and computer simulations.[10,11] For weak fluid–wall interactions liquid–vapour coexistence curves were obtained by Gibbs ensemble[10] and molecular dynamics[11] simulations and a general shift towards lower temperatures and densities was found. However the available results do not allow one to analyse the shape of the coexistence curve. For strong fluid–wall interactions layering transitions were observed in simulations of adsorption isotherms.[12,13]

Concerning water, its phase behaviour in nanopores is of special interest for biological, medical, geological and other applications. But to our knowledge there are no experimental or computer simulation results on the phase diagrams of water in pores up to now. In this paper we present for the first time fluid–fluid coexistence curves of water confined in cylindrical nanopores with smooth surfaces and various strengths of the water–substrate interaction.

TIP4P water[14] in cylindrical pores with radius $R_c = 12$ Å was simulated with periodic boundary conditions along the pore axis. The water–substrate interaction was simulated with the Lennard-Jones (9-3) potential, which depends on the distance between the oxygen atom and the pore surface only. The parameter σ of this potential was fixed at 2.5 Å, whereas the parameter ε varied to change the well-depth $U = -0.385\varepsilon$ from -0.39 to -4.62 kcal mol^{-1}. That approximately covers the range from hydrophobic (hydrocarbon-like) to hydrophilic substrates. Monte Carlo simulations in the Gibbs ensemble[10] were used to obtain water phase coexistence both in the pore and in the bulk. Typically 400 to 600 water molecules were used in the simulations. The minimal length L of the pore with the liquid phase was around 30 Å. For the vapour phase L varied from around 10^7 Å at low T to about 40 to 60 Å at high T. Using longer pores at high T for the vapour phase in the hydrophilic pore may result in the appearance of patches of the denser phase in addition to the vapour phase. This would causes an overestimation of the vapour density.

The efficiency of the deletion of molecules in the Monte Carlo moves was improved by a biased choice of more loosely bound molecules.[15] The efficiency of the insertion attempts was improved by early rejection of the new configuration if at least one of the interatomic distances between the inserted molecule and other molecules is shorter than some reference value. The acceptance probability was corrected by a factor, equal to the probability to find at random a molecule with energy higher than a chosen reference energy (in the case of deletion) or with the shortest interatomic distances, exceeding the chosen reference distances (in the case of insertion). The results obtained with and without these improvements coincide at temperatures higher 350 K, while at lower temperatures reliable results with an acceptable number of molecular transfers may be obtained by the bias methods only.

The obtained coexistence curve of the bulk TIP4P water, shown in Fig. 1(a), coincides well with available literature data for the same model.[16] The efficient technique for the molecular transfers allowed us to extend the simulation of the coexistence curve below 300 K. The liquid branch exhibits a pronounced density maximum at about 250 K, reproducing the well known temperature shift of the TIP4P model for this anomaly of water.[17]

The liquid–vapour coexistence curves of water in the pore with $U = -0.39$ and -3.08 kcal mol^{-1} are shown in Fig. 1(b) (the densities were calculated assuming that the accessible volume for water is a cylinder with radius $R = R_c - \sigma/2$). The general shift of the two-phase region to lower temperatures with strengthening water–substrate interaction is accompanied by sharp changes of the shape of the coexistence curve. Still stronger water–substrate interactions cause a splitting of

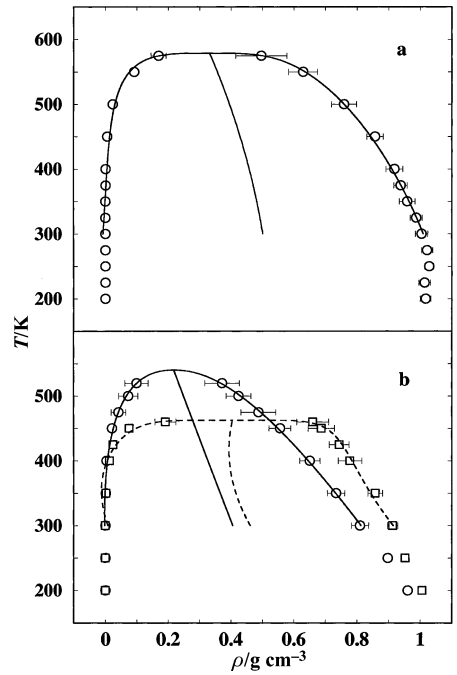

Fig. 1 Liquid–vapour coexistence curves of the bulk water (a) and water confined in cylindrical pores (b). Circles: $U = -0.39$ kcal mol^{-1}. Squares: $U = -3.08$ kcal mol^{-1}. The lines represent fits of the order parameter to eqn. (1) and of the diameter to a quadratic regression.

the liquid–vapour coexistence curve into two (Fig. 2(a), $U = -3.85$ kcal mol^{-1}) or even three regions (Fig. 2(b), $U = -4.62$ kcal mol^{-1}).

Water density distributions along the pore radius are presented in Fig. 3 for the pore with $U = -4.62$ kcal mol^{-1} and for three pairs of coexisting states along each of the three coexistence regions. It is clearly seen, that the first (I) and second (II) coexistence region corresponds to subsequent layering transitions, and the third one (III) is the liquid–vapour transition of the inner water, situated near the pore axis.

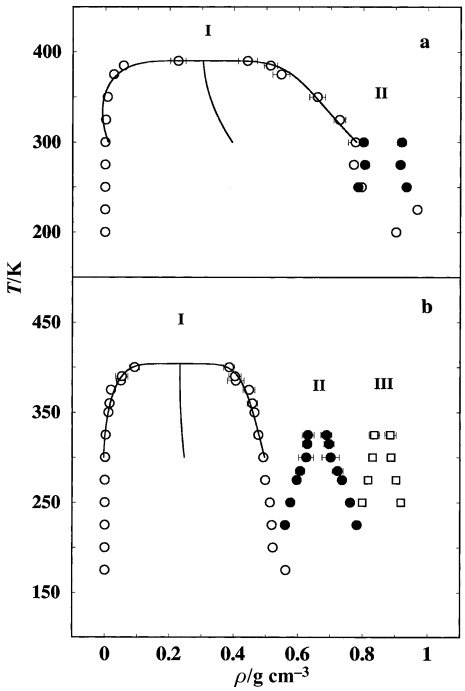

Fig. 2 Phase diagrams of water in cylindrical pores with $U = -3.85$ kcal mol^{-1} (a) and $U = -4.62$ kcal mol^{-1} (b). The lines represent fits of the order parameter to eqn. (1) and of the diameter to a quadratic regression.

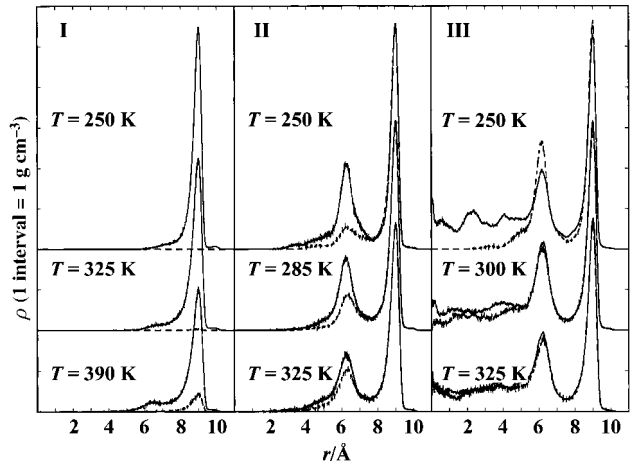

Fig. 3 Water density distributions along the pore radius for three pairs of coexisting states along each of the three coexistence regions, shown in Fig. 2(b). The coexisting phases are distinguished by solid and dashed lines.

Slight weakening of the water–substrate interaction ($U = -3.85$ kcal mol^{-1}) causes merging of the two layering transitions (see Fig. 2(a)). In the low temperature region of Fig. 2(a) only a liquid–vapour coexistence was observed. This may suggest the existence of a triple point near $T = 250$ K and $\rho = 0.8$ g cm^{-3}. Phase diagrams with a triple point, where liquid, vapour and surface layers coexist, were recently obtained for an associating Lennard-Jones fluid in a slit-like pore by a density functional method.[18]

In order to estimate the temperature range of the two-phase coexistence region, which is limited by a pore critical temperature T_c, and to analyse the shape of the coexistence curve, the order parameter $\Delta\rho = \rho_1 - \rho_2$ was fitted to the simple scaling equation

$$\Delta\rho = B\tau^{\beta_{\text{eff}}}, \quad (1)$$

ρ_1 and ρ_2 are the densities of the coexisting phases, $\tau = (T_c - T)/T_c$ and β_{eff} is an effective critical exponent. In the case of real bulk fluids the critical exponent β_{eff} approaches the 3D Ising value $\beta = 0.326$[19] in a narrow asymptotic range near T_c. More distant from the critical point corrections to the scaling equation should be taken into account. Up to 5 corrections terms are necessary to obtain a good fit of the bulk water coexistence curve in a wide temperature range.[20] However, in the same temperature range the value β_{eff}, obtained from the one-term fit (1) deviates from the asymptotic Ising value not more than 10%. This allows us to use the value of β_{eff} for a qualitative analysis of the shape of the coexistence curve. In order to compare the coexistence curves of bulk and confined water we limited the fitting range to temperatures above 300 K. The values of T_c and β_{eff} obtained from the fits of eqn. (1) to the coexistence densities (which are averaged over the entire pore) are shown in Table 1.

The decrease of the liquid–vapour critical temperature in the pores with respect to the bulk value achieves 30–35% and agrees with experimental results for cylindrical pores of the same size.[3] The exponent β_{eff} continuously decreases from 0.46 in the hydrophobic pore ($U = -0.39$ kcal mol^{-1}) to 0.16 in the hydrophilic pore ($U = -3.08$ kcal mol^{-1}), corresponding to the flattening of the coexistence curve.

As the fluid in the cylindrical nanopore is strongly spatially heterogeneous along the pore radius, we analysed the variation of β_{eff} along the pore radius. To do so, the water density was averaged over cylindrical shells with a width of 2 Å, and values β_{eff} were determined as function of the middle radius of the shells with T_c fixed to the value obtained for the entire pore. The variation of β_{eff} along the radius of the hydrophobic pore ($U = -0.39$ kcal mol^{-1}) is shown in Fig. 4. The observed sharp increase of β_{eff} towards the pore surface shows

Table 1 The parameters obtained from the fits to eqn. (1) of the coexistence curves of bulk water and water in pores with 12 Å radius for different strength U of the water–substrate interaction: T_c and β_{eff} are the critical temperature and effective critical exponent obtained from the fits of the averaged pore densities; β_s and β_i are the exponents derived from the fitting of the densities in the surface layer and inner water, respectively. For the systems with layering transitions (Fig. 2) this refers to transition I only (indicated by the asterisks)

U/kcal mol^{-1}	T_c/K	β_{eff}	β_s	β_i
Bulk water	578.6 ± 2.5	0.27 ± 0.01	—	0.27 ± 0.01
−0.39	540.4 ± 5.3	0.46 ± 0.03	0.71 ± 0.04	0.29 ± 0.03
−1.93	520.7 ± 2.7	0.27 ± 0.01	0.32 ± 0.02	0.23 ± 0.01
−3.08	462.4 ± 1.0	0.16 ± 0.01	0.18 ± 0.01	0.15 ± 0.01
−3.85*	390.2 ± 0.4	0.20 ± 0.02	0.14 ± 0.02	—
−4.62*	403.6 ± 3.6	0.16 ± 0.03	0.19 ± 0.02	—

a more rapid decrease of the density difference between the two coexisting states near the surface. In order to compare the pores with different values of U we determined separately the values β_{eff} for the water in the surface layer (7.5–12 Å) and for the inner water near the pore axis (0–4 Å), and obtained the results given in Table 1. In the hydrophobic pore ($U = -0.39$ kcal mol^{-1}) the exponent for the surface layer $\beta_{eff} = 0.71$ is close to the value of the 3D surface exponent 0.78, describing the temperature induced disordering of the semi-infinite Ising lattice near a free surface,[21] whereas it becomes closer to the 3D bulk Ising exponent for the inner water. With increasing water–substrate interaction two prominent water layers with strong orientational ordering are formed near the pore surface.[15] This structuring effectively suppresses the molecular exchange along the pore radius. As a result the water in the surface layer gets features of two-dimensionality. So, we attribute the observed decrease of β_{eff} in the surface layer with a strengthening water–substrate interaction (Table 1) to the crossover towards a 2D behaviour, which is characterized by the exponent $\beta = 0.125$.

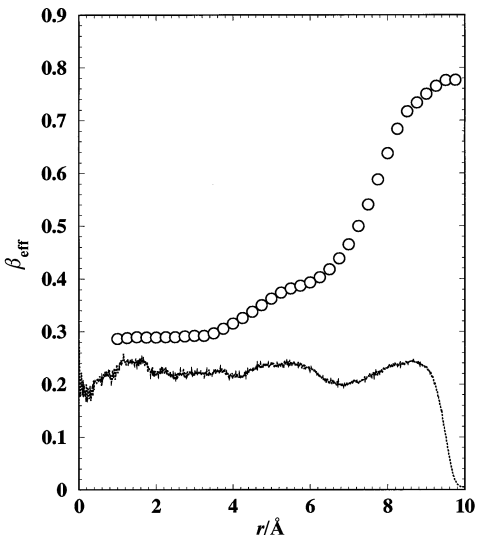

Fig. 4 Variation of the effective critical exponent β_{eff} along the radius of the pore with $U = -0.39$ kcal mol^{-1} (circles). The location of the symbols corresponds to the center of the cylindrical shells of 2 Å width, which are used for density averaging. In the lower part, the water density distribution along the pore radius is shown for the high density state at $T = 300$ K (in arbitrary units).

The observed sharp crossover from 3D surface to 2D behaviour in the surface water layer causes the appreciable changes of β_{eff}, obtained for the whole pore, as in the considered cylindrical nanopores with $R_c = 12$ Å the surface layer contains up to 60% of all molecules in the liquid phase.

It is expected that layering transitions are of the 2D Ising universality class.[1] The low values of β_{eff}, obtained by us for the layering transitions in the pores with $U = -3.85$ and -4.62 kcal mol^{-1} (see Table 1), reflect the trend towards two dimensionality.

The presented results show the necessity to take into account the rich phase behaviour of confined water in the analysis of experimental results and in computer simulations. The obtained variety of the shape of the liquid–vapour coexistence curve is the result of surface effects, which dominate in nanopores.

Acknowledgements

The elucidating criticism of M. E. Fisher, and discussions with D. P. Landau and A. Z. Panagiotopoulos are gratefully acknowledged. This work was supported by Ministerium für Schule und Weiterbildung, Wissenschaft und Forschung des Landes Nordhrein-Westfalen.

References

1 L. D. Gelb, K. E. Gubbins, R. Radhakrishnan and M. Sliwinska-Bartkowiak, *Rep. Prog. Phys.*, 1999, **62**, 1573.
2 K. Morishige and M. Shikimi, *J. Chem. Phys.*, 1998, **108**, 7821.
3 C. G. V. Burgess, D. H. Everett and S. Nuttall, *Pure Appl. Chem.*, 1989, **61**, 1845.
4 A. P. Y. Wong and M. H. W. Chan, *Phys. Rev. Lett.*, 1990, **65**, 2567.
5 A. P. Y. Wong, S. B. Kim, W. I. Goldburg and M. H. W. Chan, *Phys. Rev. Lett.*, 1990, **70**, 954.
6 M. Tommes and G. H. Findenegg, *Langmuir*, 1994, **10**, 4270.
7 S. Gros and G. H. Findenegg, *Ber. Bunsen-Ges. Phys. Chem.*, 1997, **101**, 1726.
8 V. Privman and M. Fisher, *J. Stat. Phys.*, 1983, **33**, 335.
9 R. Evans, U. Marini Bettolo Marconi and P. Tarazona, *J. Chem. Soc., Faraday Trans.*, 1986, **82**, 1763.
10 A. Z. Panagiotopoulos, *Mol. Phys.*, 1987, **62**, 701.
11 B. K. Peterson, K. E. Gubbins, G. S. Heffelfinger, U. Marini Bettolo Marconi and F. Van Swol, *J. Chem. Phys.*, 1988, **88**, 6487.
12 P. C. Ball and R. Evans, *J. Chem. Phys.*, 1988, **89**, 4412.
13 B. K. Peterson, G. S. Heffelfinger, K. E. Gubbins and F. van Swol, *J. Chem. Phys.*, 1990, **93**, 679.
14 W. L. Jorgensen, J. Chandrasekhar, J. D. Madura, R. W. Impey and M. L. Klein, *J. Chem. Phys.*, 1983, **79**, 926.
15 I. Brovchenko, D. Paschek and A. Geiger, *J. Chem. Phys.*, 2000, **113**, 5026.
16 J. Vorholz, V. I. Harismiadis, B. Rumpf, A. Z. Panagiotopoulos and G. Mauer, *Fluid Phase Equilibria*, 2000, **170**, 203.
17 F. Sciortino, P. H. Poole, U. Essmann and H. E. Stanley, *Phys. Rev. E*, 1997, **55**, 727.
18 A. Huerta, O. Pizio and S. Sokolowski, *J. Chem. Phys.*, 2000, **112**, 4286.
19 R. Guida and J. Zinn-Justin, *J. Phys. A, Math. Gen.*, 1998, **31**, 8103.
20 Y. Guissani and B. Guillot, *J. Chem. Phys.*, 1993, **98**, 8221.
21 K. Binder, in *Phase Transitions and Critical Phenomena*, ed. C. Domb and J. L. Lebowitz, Academic, London, 1983, vol. 8, p. 1.